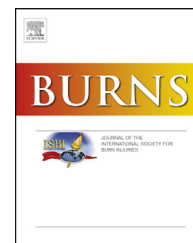


Available online at www.sciencedirect.com

ScienceDirect

journal homepage: www.elsevier.com/locate/burns

Development of dynamic cell and organotypic skin models, for the investigation of a novel visco-elastic burns treatment using molecular and cellular approaches

Robert G. Wallace^{a,1}, Mary-Rose Kenealy^{a,1}, Aidan J. Brady^a,
 Laura Twomey^{a,b}, Emer Duffy^c, Bernard Degryse^{a,d},
 David Caballero-Lima^e, Niall M. Moyna^a, Marc-Antoine Custaud^f,
 Gerardene Meade-Murphy^g, Aoife Morrin^c, Ronan P. Murphy^{a,d,*}

^a Center for Preventive Medicine, School of Health & Human Performance, Dublin City University, Dublin 9, Ireland

^b Technological University Dublin, Ireland

^c School of Chemical Sciences, Dublin City University, Dublin 9, Ireland

^d Integrative Cell & Molecular Physiology Group, School of Health & Human Performance, Dublin City University, Dublin 9, Ireland

^e LabSkin, Innovenn, UK & Ireland

^f Centre de Recherche Clinique du CHU d'Angers, Angers, France

^g Department of Pharmacology and Therapeutics, University College Cork, Cork, Ireland

ARTICLE INFO

Article history:

Accepted 28 April 2020

Keywords:

Emergency burn dressing
 Organotypic modelling of burns
 Real-time cellular analysis
 Burn wound healing
 Cell & molecular
 Comparative transcriptomics

ABSTRACT

Background: Burn injuries are a major cause of morbidity and mortality worldwide. Despite advances in therapeutic strategies for the management of patients with severe burns, the sequelae are pathophysiologically profound, up to the systemic and metabolic levels. Management of patients with a severe burn injury is a long-term, complex process, with treatment dependent on the degree and location of the burn and total body surface area (TBSA) affected. In adverse conditions with limited resources, efficient triage, stabilisation, and rapid transfer to a specialised intensive care burn centre is necessary to provide optimal outcomes. This initial lag time and the form of primary treatment initiated, from injury to specialist care, is crucial for the burn patient. This study aims to investigate the efficacy of a novel visco-elastic burn dressing with a proprietary bio-stimulatory marine mineral complex (MXC) as a primary care treatment to initiate a healthy healing process prior to specialist care. **Methods:** A new versatile emergency burn dressing saturated in a >90% translucent water-based, sterile, oil-free gel and carrying a unique bio-stimulatory marine mineral complex (MXC) was developed. This dressing was tested using LabSkin as a burn model platform. LabSkin a novel cellular 3D-dermal organotypic full thickness human skin equivalent, incorporating fully-differentiated dermal and epidermal components that functionally models skin. Cell and molecular analysis was carried out by *in vitro* Real-Time Cellular Analysis (RTCA), thermal analysis, and focused transcriptomic array profiling for

* Corresponding author at: School of Health & Human Performance, Faculty of Science and Health, Dublin City University Glasnevin, Dublin 9, Ireland.

E-mail address: ronan.murphy@dcu.ie (R.P. Murphy).

¹ First named authors, equal contribution.

<https://doi.org/10.1016/j.burns.2020.04.036>

0305-4179/© 2020 Elsevier Ltd and ISBI. All rights reserved.

This is an open access article under the CC BY license (<http://creativecommons.org/licenses/by/4.0/>).

quantitative gene expression analysis, interrogating both wound healing and fibrosis/scarring molecular pathways. *In vivo* analysis was also performed to assess the bio-mechanical and physiological effects of this novel dressing on human skin.

Results: This hybrid emergency burn dressing (EBD) with MXC was hypoallergenic, and improved the barrier function of skin resulting in increased hydration up to 24 h. It was demonstrated to effectively initiate cooling upon application, limiting the continuous burn effect and preventing local tissue from damage and necrosis. xCELLigence RTCA® on primary human dermal cells (keratinocyte, fibroblast and micro-vascular endothelial) demonstrated improved cellular function with respect to tensegrity, migration, proliferation and cell-cell contact (barrier formation) [1]. Quantitative gene profiling supported the physiological and cellular function finding. A beneficial *quid pro quo* regulation of genes involved in wound healing and fibrosis formation was observed at 24 and 48 h time points.

Conclusion: Utilisation of this EBD + MXC as a primary treatment is an effective and easily applicable treatment in cases of burn injury, proving both a cooling and hydrating environment for the wound. It regulates inflammation and promotes healing in preparation for specialised secondary burn wound management. Moreover, it promotes a healthy remodelling phenotype that may potentially mitigate scarring. Based on our findings, this EBD + MXC is ideal for use in all pre-hospital, pre-surgical and resource limited settings.

© 2020 Elsevier Ltd and ISBI. All rights reserved.

1. Introduction

The American Burns Association states that nearly half a million Americans receive medical treatment for burn-related injuries in the United States annually, with approximately 3400 deaths being attributed to such injuries [2]. Of 40,000 hospital admissions for burns, 30,000 are to specialised burn centres [3], as burns are one of the most complex acute wounds to treat [4–7]. Survival rates for admitted burn patients has consistently improved over the past decennia [8,9] and currently stands at 97% for patients admitted to burn centres [6]. This can be largely attributed to major advances in therapeutic strategies for the management of patients with severe burns, including improved resuscitation, improved and enhanced wound coverage, infection control, fluid management, and management of inhalation injuries [10–12]. These clinical advancements in primary critical burn care, burn wound care and treatment have been primarily driven forward by active research in this field, with such studies leading to vital improvements in many areas of specialised burn care. Management of patients with severe burn injuries requires long-term integrated and synergistic care, a programme that specifically addresses the burn wound as well as the systemic, psychologic, and social consequences of the injury [13–15].

The primary intervention and management stage of a critical burn wound, prior to specialised burns care, is crucial to a favourable outcome with respect to morbidity and mortality [14]. This is emphatically true in situations where resources are limited and/or over-stretched, as seen in mass casualties due to natural disaster, terrorist attack, theatres of conflict, and large accidents [16,17]. Severe burns occur in approximately 5–20% of survivors of conventional conflicts and from civilian mass disasters or terrorist events [8,18–22]. However, due to limited or inadequate resources to care for large numbers of severely burned individuals, or those in isolated remote areas, the majority of large (>20%) total burn surface area (TBSA) burn patients die at the scene or within the first

24 h following the burn [8,23–26]. With appropriate protocols and disaster plans in place, a state-of-the-art burn centre can typically handle a surge capacity $\leq 50\%$ above normal maximum capacity. Such catastrophes may also delay transportation of the burn victim to a specialised medical setting. In such events, appropriate and comprehensive primary care is essential while effective and rapid triage, stabilisation, and transfer provide optimal outcomes. However outcomes for severely burned patients, particularly children or the elderly, who cannot be transferred for burn care, are poor [27–31].

Despite advances, concerns for the success, time and cost of treatment, inability to restore functionality of the skin, and the high rates of complications related to severe burn wounds remain [32]. This has led to an increased focus on developing ‘smart’ wound dressings [33–38] and regenerative approaches [39,40]. Deep partial- and full-thickness burns heal slowly when standard wound care alone is performed. Development of advanced wound dressings is crucial to improved primary wound care, because it not only protects the wound, but also offers the opportunity to cool and preserve damaged tissue, initiating a healing and regenerative environment for wound closure.

In order to meet this challenge, a new versatile visco-elastic emergency burn dressing (EBD) saturated in a >90% translucent water-based, sterile, oil free gel and carrying a unique bio-stimulatory marine mineral complex (MXC) was developed (EBD + MXC). Natural bio-stimulatory formulations for the treatment of these lesions, have been increasingly studied for applications in health care due to their biocompatibility, biodegradability, and non-cytotoxicity [33,41–45]. As our understanding of the cellular and molecular basis of wound healing, and the pathophysiology of fibrosis and chronic wounds has increased, the importance of minerals in this process is becoming accepted and recognised globally [46–49].

The goal of this study was to validate this novel dressing and assess its ability to provide spontaneous cooling, anti-fibrosis, pro-healing activity and reducing the *nidus* for the improved treatment of burns prior to specialised care. To this

end we developed and employed a range of humanised *in vitro* cell models to study the molecular and cellular responses to thermal injury and to assess the efficacy of EBD + MCX as an optimal and functional primary dressing. These included utilising a novel cellular 3D-dermal organotypic burn model platform, *in vitro* Real-Time Cellular Analysis (RTCA) [50–57], thermal analysis, and focused transcriptomic array profiling for quantitative gene expression analysis. *In vivo* analysis was also performed to assess the bio-mechanical and physiological effects of this novel dressing on human skin.

2. Materials & methods

2.1. *In vitro* cytotoxicity testing

Testing methodology was based on principles derived from the International Organisation for Standardisation (ISO) in order to assess *in vitro* cytotoxicity of medical devices. Multiple cultures of L-929 mammalian fibroblast cells in a serum-supplemented minimum essential medium (MEM) were prepared. Cultures were incubated at 37 (± 1)°C in a 5 (± 1)% CO₂ atmosphere, with final addition of culture medium containing a final mass concentration of agar of 0.5%–2%. This agar layer was thin enough to permit diffusion of any leached chemicals/bio-actives. The test article (0.1 mL on 1 cm² sterile filter paper), negative (physiological buffered saline, 0.1 mL on 1 cm² filter paper) and positive (1 cm² latex) controls were placed in triplicate cultures such that they were in contact with the solidified agar. The surface area of the articles placed on the agar was 10 mm². Three wells received agar only as blank controls. All cultures were then incubated for 24 h at 37 (± 1)°C as before. After 24 h, wells were examined by microscopy. Biological reactivity (cellular degeneration and malformation) was described and rated on a scale of 0–4.

In addition to the traditional ISO assay, cytotoxicity of the active ingredient (MCX) was assayed over a range of concentrations using xCELLigence[®] real-time cell analysis (RTCA), allowing cells to be continuously monitored in the absence of labels [57]. Cell cultures (Human Primary Dermal (i) Fibroblast or (ii) Keratinocytes) were incubated at 37 (± 1)°C in a 5 (± 1)% CO₂ atmosphere. Prepared cultures were brought to quiescence by serum-starvation for 24 h prior to initiation of experiments. Cells were seeded (30,000 cells/well) onto wells of an E-Plate 16[®] (ACEA Biosciences Inc., USA) for adhesion experiments. E-Plates[®] are single-use, disposable devices used for performing cell-based assays on the xCELLigence[®] system. Each individual well on an E-Plate[®] incorporated a sensor electrode array, allowing cells to be monitored and assayed in real time through the measurement of electrical impedance. An initial sweep was used to eliminate background noise before beginning the assay. The subsequent programme consisted of 96 sweeps at 15 min intervals. This enabled real-time monitoring over a 24 h period.

2.2. *In vivo* skin irritation testing

This study met the requirements of U.S. FDA GLP: 21 CFR Part 58, 1987, compatible with OECD Principles of GLP (as revised in

1997): ENV/MC/CHEM(98)17, OECD, Paris, 1998. All animal experiments strictly comply with the ARRIVE guidelines and were carried out in accordance with the U.K. Animals (Scientific Procedures) Act, 1986 and associated guidelines, EU Directive 2010/63/EU for animal experiments, and the National Institutes of Health guide for the care and use of Laboratory animals (NIH Publications No. 8023, revised 1978). In order to assess the potential of skin irritation from a single topical exposure to EBD + MXC, a skin irritation test was carried out through a semi-occlusive application. The test article (EBD + MXC) was applied on the intact skin of 3 healthy, naive rabbits (not previously tested) without pre-existing skin irritation, to the dorsal region both on the left and on the right side for 4 h. Each animal had the right caudal region and left cranial region treated with EBD + MXC and the left caudal region and right cranial region used as control sites. 6-cm² dose sites were evaluated for erythema and edema approximately 1 h following removal of patches and again evaluated 24, 48 and 72 h after treatment. All animals were active and healthy during the study. No signs of gross toxicity, adverse clinical effects, or abnormal behaviour were observed. The test article (EBD + MXC) was administered in a single dose by topical application (recommended in the referenced guidelines and because human exposure would occur *via* this route). General procedures associated with the balanced design and conduct of this study were employed to control bias.

2.3. Cumulative irritation and/or allergic contact sensitisation: *in vivo* human study

This trial (Study Number CIS-4085.01) was conducted in accordance with the Declaration of Helsinki, the ICH Guideline E6 for *Good Clinical Practice*, the requirements of 21 CFR Parts 50 and 56, other applicable laws and regulations, CPTC Standard Operating Procedures, and the approved protocol. Two hundred and twenty-seven (227) qualified subjects, male and female, ranging in age from 18 to 70 years, were selected for this evaluation. Two hundred and seventeen (217) subjects completed this study. Remaining subjects discontinued their participation for various reasons, none of which were related to the application of the test material. Inclusion criteria were as follows; (i) male and female subjects, age 16–79 years, (ii) absent of any visible skin disease which could be confused with a skin reaction from the test material, (iii) prohibition of use of topical or systemic steroids and/or antihistamines for at least seven days prior to study initiation, (iv) completion of a Medical History Form and the understanding and signing of an Informed Consent Form and (v) considered reliable and capable of following directions. Exclusion criteria were as follows; (i) ill health, (ii) under a doctor's care or taking medication(s) which could influence the outcome of the study, (iii) Females who were pregnant/nursing and (iv) a history of adverse reactions to cosmetics or other personal care products.

The upper back between the scapulae served as the treatment area. Approximately 0.2 mL of test material (EBD + MXC), or an amount sufficient to cover the contact surface, was applied to the 1 inch \times 1 inch absorbent pad portion of a clear adhesive dressing. This was then applied to the appropriate treatment site to form a semi-occlusive patch.

Patches were applied 3 times per week for a total of 9 applications.

2.4. Application of thermal injury to *in vitro* 3D models

In vitro burn insults were applied to 3D LabSkin full thickness human skin equivalent models using a modified animal model protocol by Cai *et al.* [58]. LabSkin was obtained from Innovenn Ltd. (York, England). Custom weights were milled from brass stock. Weights were heated on a heating block (Stuart) and temperature checked using an infrared thermometer. Models (in well-insert baskets) were removed from 6-well plates and quickly placed onto a plastic surface in a sterile laminar cabinet to avoid heat dissipation as the burn was applied (15 s). Immediately following the burn, weights were removed and the appropriate treatment was topically applied. Each treatment consisted of custom-fitted 2.5 cm gauze disks soaked in the appropriate therapy. Models were returned to the incubator for 24 and 48 h, after which time, models were sampled for subsequent analysis. Skin biopsies were taken from the model using Integra[®] 3 mm disposable biopsy punches (Fisher Scientific Ltd.) post-treatment. Samples were immediately snap-frozen in liquid Nitrogen, before storage at -80°C . For running water comparisons, a custom-designed waterproof heating apparatus was constructed to simulate core temperature of $37(\pm 1)^{\circ}\text{C}$ during the experiment. Water delivery was controlled at flow rate of 0.2 L/min from a reservoir of tap water, temperature range $21 (\pm 1)^{\circ}\text{C}$.

2.5. Stratum corneum hydration measurements

Healthy volunteers were recruited (2 males age 22 and 26, 1 female age 27) for skin hydration measurements. Stratum corneum (SC) hydration was measured using a GPSkin[®] Barrier probe (GPOWER Inc, Seoul, South Korea) which measures bioelectrical impedance at a frequency of 1 kHz. Skin was characterised over a 24-h period, where measurements were made 0, 1, 2, 4, 8 and 24 h after application of EBD, MXC, EBD + MXC and control gel to the volar forearm. An adjacent skin site was also measured as a control over the 24-h period. Each measurement was repeated 3 times. The sensor probe was cleaned with alcohol wipes (Cutisoft wipes, BSN medical GmbH, Hamburg, Germany) and dried between measurements.

2.6. Real time cellular analysis of primary human dermal fibroblasts and primary human dermal keratinocytes using real time cellular analysis (RTCA)

Cell cultures (Human Primary Dermal (i) Microvascular Endothelial, (ii) Fibroblast or (iii) Keratinocytes) were incubated at $37 (\pm 1)^{\circ}\text{C}$ for 24 h in a $5 (\pm 1)\%$ CO_2 atmosphere, until a monolayer, with a confluence of approximately 80% was obtained. Prepared cultures were brought to quiescence by serum-starvation for 24 h prior to initiation of experiments. Cells were seeded (30,000 cells/well) onto E-Plate 16[®] (ACEA Biosciences Inc., USA) for adhesion experiments. E-Plates[®] are single-use, disposable devices used for performing cell-based assays on the xCELLigence[®] system. Each individual well on an E-Plate[®] incorporates a sensor electrode array, allowing

cells to be monitored and assayed in real time through the measurement of electrical impedance. An initial sweep was used to eliminate background noise before beginning the assay. The subsequent programme consisted of 96 sweeps at 15 min intervals. This allowed real-time monitoring of adhesion over a 24 h period.

2.7. Wound healing cell migration assay

The *in vitro* wound healing assay is a simple method based on the principle that upon creation of an artificial gap in a confluent monolayer of cells, those cells on the edge of the gap will migrate/proliferate toward the opening to close the “wound” until new cell–cell contacts are established [59]. Confluent monolayers of cells were scratched with a sterile 200 μL pipette tip using firm, even pressure. Cells were washed with warm PBS, removing damaged cells and debris, before adding the treated medium. A Leica DM500 microscope with ICC50 camera module was used to capture $40\times$ images at 6 h regular intervals during wound closure, with Image J software (National Institutes for Health, USA) and the Angiogenesis Analyzer macro plugin subsequently used to determine the rate by measuring the changes in the gap area. Measurements were reported in pixels.

2.8. Angiogenic tube formation assay

The tube formation assay is a tool for angiogenesis quantification. It is based on the principle that cells differentiate morphologically to form capillary-like tubes within 24 h by first adhering to a substrate and then migrating towards each other. MaxGel[™] ECM (Sigma Aldrich) was thawed slowly on ice overnight, before pre-coating Ibidi[®] Angiogenesis μ -slides and allowed to solidify at 37°C in a sterile incubator. This formed a basement membrane-like surface in each 4 mm well. A 50 μL 2×10^5 cells/mL HAEC suspension was subsequently used to seed on top of this. Cells were observed and imaged in 6-h intervals. A Leica DM500 microscope with ICC50 camera module was used to capture $100\times$ images at 6 h regular intervals during this process, with Image J (National Institutes for Health, USA) software and the MRI Wound Healing Tool.ijm macro plugin subsequently used to quantify the rate by measuring tube length. Measurements were reported in pixels.

2.9. RNA isolation

Tissue samples were homogenised in QIAzol Lysis Reagent[®], and RNA was isolated using the RNeasy Plus Universal Kit[®] (QIAGEN, Cat.No. 73404). This utilised a spin column-based protocol to facilitate separation and eliminate phenol and other contaminants. RNA quality and concentration were subsequently determined using a Nanodrop[™] spectrophotometer to measure the concentration and OD260/280 values of the samples, while Agilent RNA TapeScreen[®] was employed

to check RNA quality. For the integrity measurement, 1 μ L of the total RNA was analysed with a RNA ScreenTape using an Agilent TapeStation™.

2.10. Gene analysis methods

Quantitative real-time reverse transcription polymerase chain reaction (qRT-PCR) was used to analyse gene expression. The Qiagen RT² First Strand Kit (Catalog # 330401) was used for cDNA synthesis and was designed to work in tandem with Qiagen RT² profiler arrays. RT² Profiler PCR Arrays facilitated analysis of gene panels related to wound healing, fibrosis and associated biological pathways. Following qRT-PCR, relative expression was determined using the $\Delta\Delta$ Ct method. The PCR Array Data Analysis Web Portal was used to interpret replicate ($n = 3$) qRT-PCR data. Any cyclic threshold (Ct) value equal to 35 was considered a negative call. RT² Profiler arrays incorporated a number of controls, including genomic and reverse transcription controls. The panel of endogenous controls were used to normalise data (Ct Gene of Interest – Ct Average of endogenous controls). Biological replicates were performed, and the average Δ Ct value of each gene was calculated across those replicate arrays for each treatment group. Calculated $\Delta\Delta$ Ct for each gene across two groups or PCR Arrays. $\Delta\Delta$ Ct = Δ Ct (group 2) - Δ Ct (group 1). In each case, Group 1 was the control and Group 2 was the experimental. Fold-change for each gene from Group 1 to Group 2 was calculated as $2^{(-\Delta\Delta$ Ct)}. If the fold-change was greater than 1, the result was reported as a fold up-regulation.

3. Results

3.1. Oral and skin toxicity, dermal inflammation and cytotoxicity assessment

Prior to the commencement of the study, a comprehensive battery of cytotoxicity and inflammation assays were performed, results of which are outlined in Tables 1–3 (Supplementary material). To further support this data, *in vitro* and *ex vivo* assessments were carried out on primary human dermal cell lines and human platelets. Results demonstrated that MXC alone was highly biocompatible, as well as in complex (EBD + MXC). No toxicity or inflammation was observed. MXC was demonstrated to be well tolerated orally (unpublished data) as well as topically. *In vitro* analysis using xCELLigence RTCA and primary human dermal cells (Keratinocytes, Fibroblasts, microvascular (mv) Endothelial Cells) treated with varying concentrations of MXC, further demonstrated the high biocompatibility of MXC.

3.2. Skin hydration studies: *in vivo* and *in vitro* 3D-LabSkin assessment

Tissue Dielectric Constant analysis using *in vitro* 3D-LabSkin treated with EBD \pm MXC demonstrated the improved hydration up to 24 h with EBD + MXC as opposed to EBD-MXC (Fig. 1A). This observation confirmed an improved skin barrier formation with MXC treatment. *In vivo* analysis, while highlighting the inter individual responses observed due to

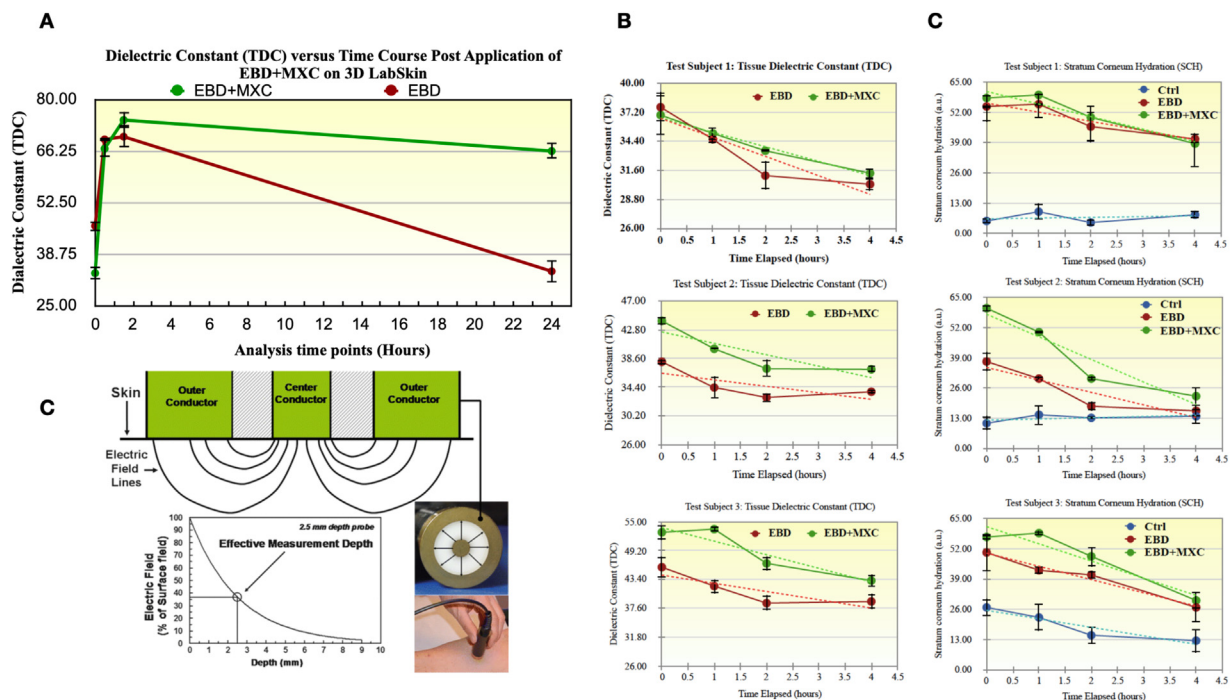


Fig. 1 – (A) Dielectric Constant (TDC) versus Time Course Post Application of EBD \pm MXC on 3D LabSkin. (B) Dielectric Constant (TDC) versus Time Course Post Application of EBD \pm MXC on *in vivo* human skin. (C) Stratum Corneum Hydration (SCH) measurements versus Time Course Post Application of EBD \pm MXC on *in vivo* human skin. (D) Apparatus used in assessing Free and Bound Water in Skin at 300 MHz Using Tissue Dielectric Constant Measurements.

environmental and biological architecture (sex, age, diet, hydration status, activity and skin friction, prior use of skin products (e.g. soaps), supported the *in vitro* analysis (Fig. 1B&C).

3.3. MXC effects on primary human dermal cells using real time cellular analysis

In order to assess the effect of both the stimulatory ingredient, MXC, and EBD Gel + MXC on human primary dermal cells, i.e. Keratinocytes and Fibroblasts, *in vitro* Real-Time Cellular Analysis (RTCA) was undertaken using novel cell modelling and analysis (Figs. 1–4). The xCELLigence® system monitors cellular events in real time without the incorporation of labels, measuring electrical impedance across integrated micro-electrodes on the bottom of tissue culture E-plates®. Electrode impedance, which is displayed as arbitrary units known as cell index (CI) values. The label free system allows for a more physiological assay which provides an optimal environment cell fate and function. By analysing the dynamic response of these cells, in an *in vitro* cellular platform of human primary skin cells, to varying concentrations of MXC, we were able to

assess multiple parameters in real-time. We determined- (1) cellular tolerance, (2) cytotoxicity, and (3) cellular response (fate and function) with respect to MXC kinetics and dynamics. Cell models of both cell types were grown on a 2.5-Dimensional of a complex Extra Cellular Matrix milieu, and cellular response assessed by impedance, enabling the study of the long term effects of MXC on both primary human dermal keratinocytes and fibroblasts. Temporal analysis, along the time axis, facilitated functional studies in relation to a number of cell fate and functions- parameters important for skin health. These included (1) cell adhesion, (2) cell activation and spreading (tensegrity), (3) cell proliferation or cell quiescence and (4) apoptosis/cytotoxicity.

3.4. Real-time cellular analysis of primary human dermal keratinocyte cells (hKC) in response to varying concentrations of MXC (0.1%–1.5%), over 48 h

Results obtained over the 48 h study highlight that the MXC is biocompatible and well tolerated up to concentrations of 1%. Fig. 2 highlights the pertinent data at concentrations of 0.1%

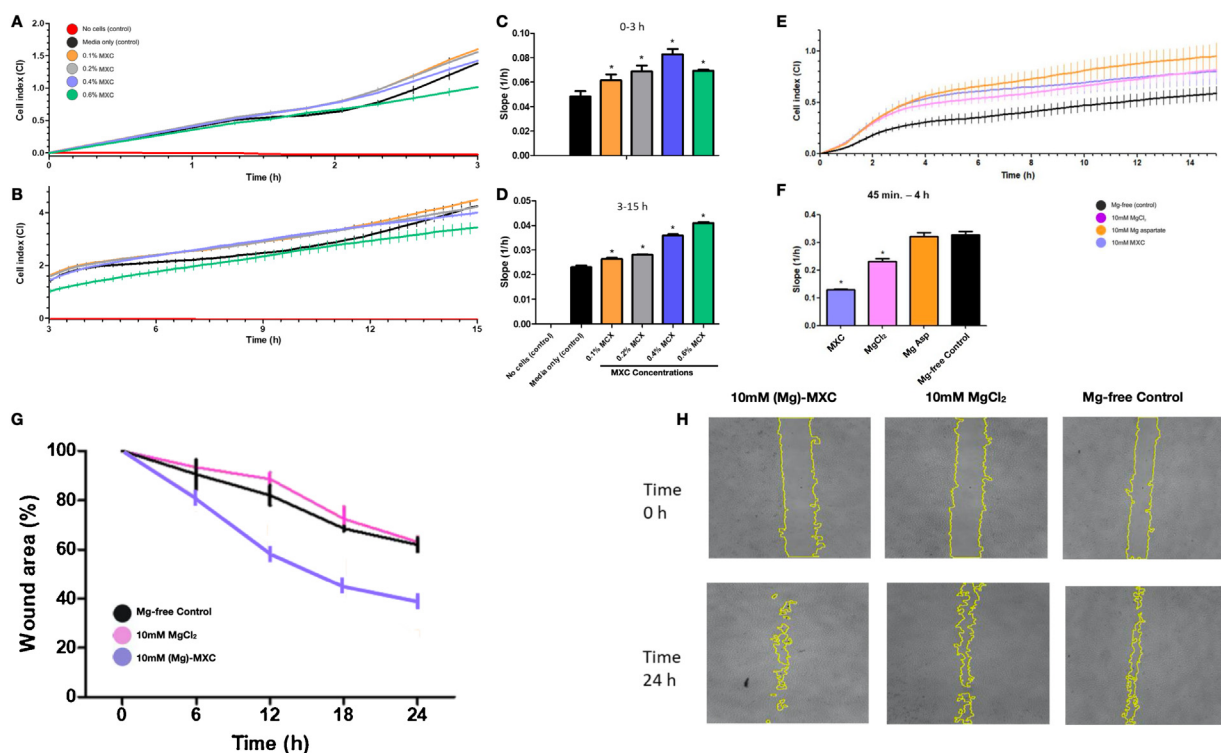


Fig. 2 – (A & B) Real-Time Cellular Analysis (RTCA) of Primary Human Adult Keratinocyte Cells (pHAKCs). Cell dynamics and function in 2.5D cell model (diluted MaxGel, 1%), in response to varying concentrations of MXC (0.1%–0.6%). Results are averaged from three independent experiments \pm SD. (C & D) Rate of cell adhesion (0–3 h) and proliferation (3–15 h) was determined by calculating the slope of the line between determined timepoints. Results are averaged from three independent experiments \pm SD; * $P \leq 0.05$ compared to media only control. (E) xCELLigence® migration profile of pHAKCs treated with different Mg forms (10 mM) for 24 h (0–15 h shown only). Static quiescent, Mg-starved pHAKCs were exposed to 10 mM Mg in a variety of common forms (Mg aspartate, MgCl₂) in addition to MXC using the xCELLigence® electrical impedance system. Results are averaged from three independent experiments ($n = 3$) \pm SD. (F) Rate of migration of HAKCs between 45 min and 4 h. Rate was determined by calculating the slope of the line between determined timepoints. Results are averaged from three independent experiments ($n = 3 \pm$ SD). * $P \leq 0.05$ vs Mg-free control. (G) Effect of 10 mM Mg on wound healing in pHAKCs represented as scratch repair rate in pHAKCs over 24 h ($n = 3$). (H) Representative images of wound healing in pHAKCs at time = 0 h and time = 24 h.

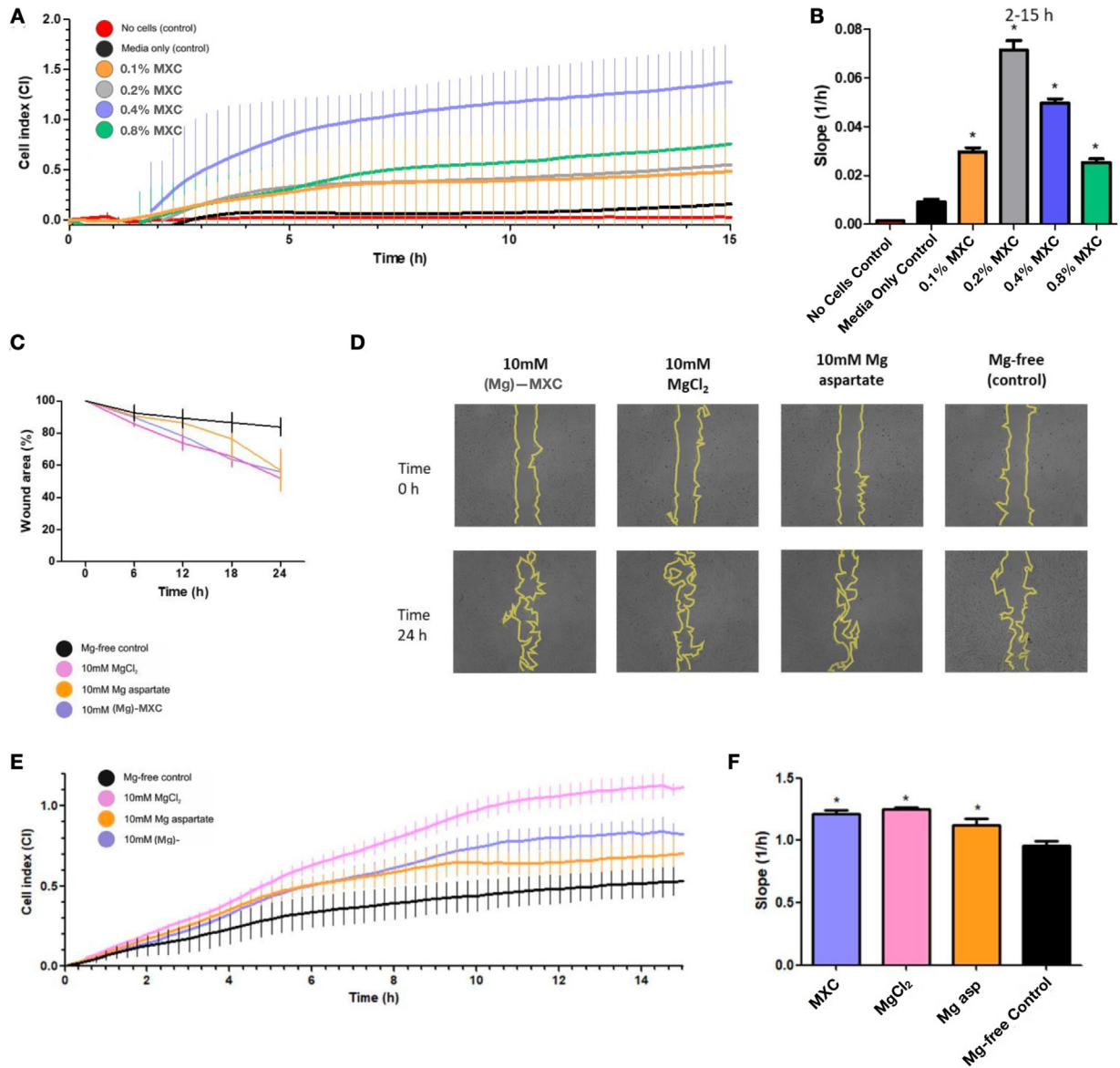


Fig. 3 – (A) Real-Time Cellular Analysis of Primary Normal Human Dermal Fibroblasts (pNHDFCs). Cell dynamics and function in 2.5D cell model (diluted MaxGel 1%), in response to varying concentrations of MXC (0.2–0.5%). Results are averaged from three independent experiments \pm SD. **(B) Rate of cell spreading and proliferation** were determined by calculating the slope of the line between determined timepoints. Averaged from three independent experiments \pm SD; * $P \leq 0.05$ versus media only control. **(C & D) Effect of 10 mM Mg (MXC, MgCl₂ on wound healing** in pNHDFCs using a scratch assay. **(E) xCELLigence[®] cell spreading, migration and proliferation profile** of pNHDFCs treated with different Mg forms (10 mM) for 24 h (0–15 h). Static quiescent, Mg-starved pNHDFCs were exposed to 10 mM Mg in a variety of common forms (Mg aspartate, MgCl₂) in addition to MXC using the xCELLigence[®] electrical impedance system. Results are averaged from three independent experiments ($n = 3$) \pm SD. **(F) Rate of spreading and migration of NHDFCs (45 min–4 h).** Rate was determined by calculating the slope of the line between determined timepoints. Results are averaged from three independent experiments ($n = 3 \pm$ SD). * $P \leq 0.05$ vs Mg-free control.

–0.6% up to 15 h for brevity). No apoptosis or cell death was observed, however cellular dynamics were arrested at concentrations close to 1.5% (data not shown), i.e. cells adhered and survived but did not spread, integrate into the extracellular matrix or proliferate (they were held in cell cycle arrest). Long term exposure studies (>24 h to 4 days) highlighted one potential beneficial effect of MXC on keratinocyte cell biology in that it appreciably slowed the rate of keratinocyte cell

proliferation, at concentrations between 0.6% and 1%, inhibiting the process. Acute analysis (0–24 h) demonstrates that MXC promotes cell attachment/adhesion, spreading and migration and proliferation at concentrations up to 0.5%, as measured by the calculation the slope between two time points of the curves, with rates levelling out at higher (>0.6%) concentrations (Fig. 2A). Furthermore, MXC stimulates primary human dermal keratinocyte cell proliferation in a

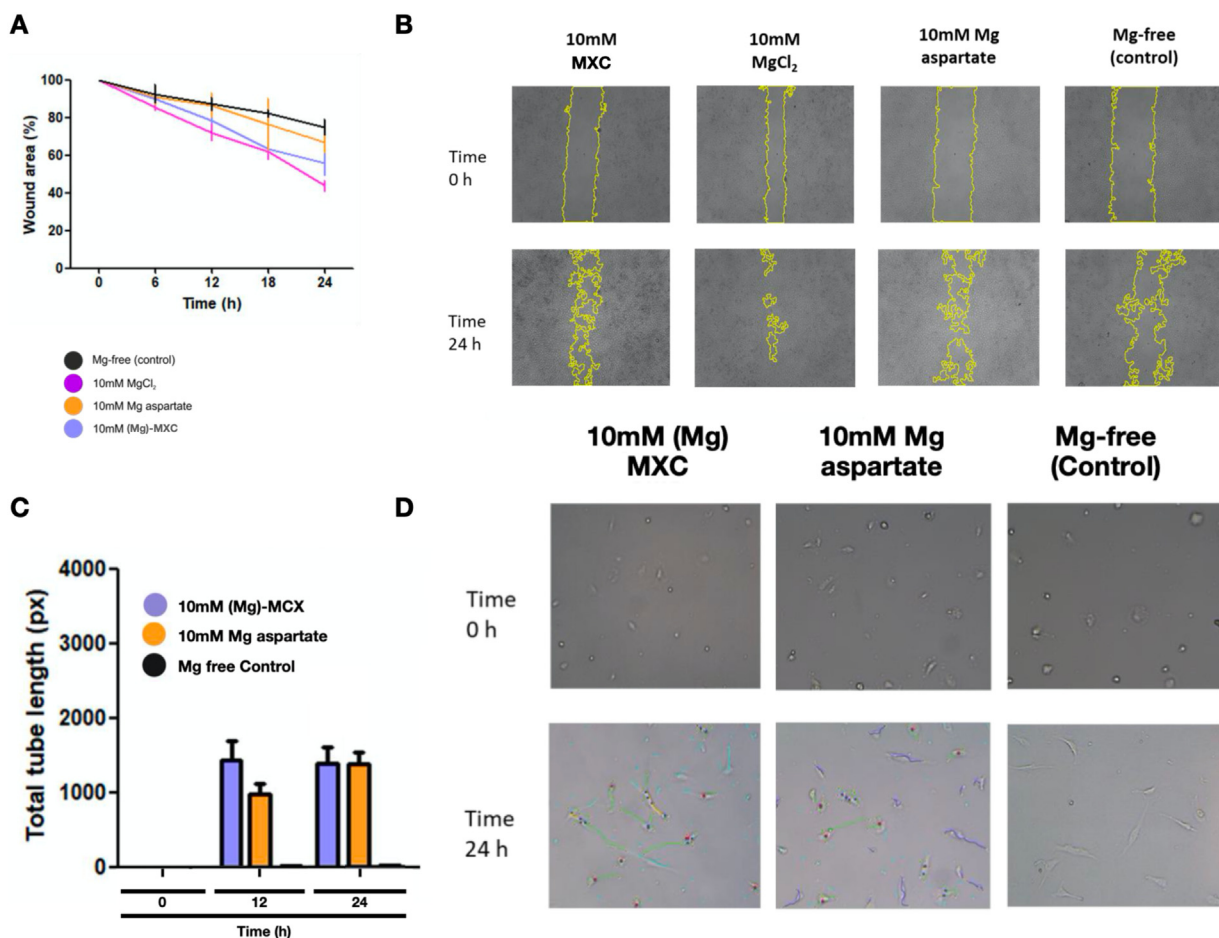


Fig. 4 – (A & B) Effect of MXC on wound healing in pHAECs. Scratch repair rate in HAECs over 24 h (n = 3). Representative images of wound healing in HAECs at time = 0 h and time = 24 h are shown. (C & D) Effect of MXC on pHAEC angiogenesis capacity- tube formation/sprouting assay. Static quiescent, Mg-starved HAECs were exposed to 10 mM Mg in a variety of common forms (Mg aspartate, MgCl₂) in addition to MXC on MaxGel™ ECM. Results are averaged from three independent experiments (n = 3) ± SD. Representative images of tube formation/sprouting in HAECs at time = 0 h and time = 24 h. Coloured lines indicate sprout/tube outline detection and signify length.

concentration dependent manner (0–0.6%) up to 24 h- data from 0 to 15 h presented in Fig. 2B. Rates of adhesion and proliferation were determined by calculating the slope of the line between timepoints. RTCA of Primary Human Dermal Keratinocytes Adhesion to 2.5 Dimension Tissue Model, in response to varying concentrations of Oriol Marine Mineral Complex (0.1%–0.6%). Fig. 2A demonstrates the cellular adhesion dynamics, mediated through KC integrin receptors, to the extracellular matrix environment. From these cellular kinetics and dynamics it was demonstrated that MXC promotes cell adhesion at three concentrations – 0.1%, 0.2% and 0.4%. At these concentrations MXC increases the rate of cell adhesion, as demonstrated by the increase in line slope, and also the final cell spreading, as indicated by the greater Cell Index (CI) at 3 h. The implications of these findings is that MXC has the potential to improve skin tone/barrier and biomechanics by increasing and improving the biological process known as Cellular Tensegrity [1,60–62]. Concentrations of MXC at >1–1.5% greatly reduces the rate

of adhesion and cell spreading, but does not reduce cell viability. Concentrations of MXC at both 0.6% and 0.8%, modestly reduce cell spreading when compared to control keratinocytes (media and cells only), but has no effect on cell adhesion dynamics and kinetics (i.e. formation of Focal Contacts, Focal Complexes and Focal Adhesions) when compared to control (Fig. 2A–D).

Graphical representation of cell adhesion, spreading and proliferation dynamics are outlined in Fig. 2, which represents the Keratinocyte cell-ECM adhesion turnover (making and breaking of cell interactions). It can be seen that MXC promotes cell adhesion formation above and beyond that of Control, between 4.5 h and 15 h- at three concentrations – 0.1%, 0.2% and 0.4%. MXC at concentrations of 0.6% and 0.8% slightly reduces the rate of adhesion formation, but only modestly when compared to control cells. The response observed for MXC at 0.1%, 0.2% and 0.4%, is indicative of increased cell spreading (activation of the GTPase –RAC1) and this increase in Focal Contact, Focal Complex and Focal Adhesion formation

is a highly dynamic process, highlighting the bio-stimulatory capacity of MXC. It can be observed that control Keratinocytes loose traction within the ECM complex between 4.5 h and 12.5 h (reduction in Cell Index), while it is maintained at 0.1%, 0.2% and 0.4% of MXC. Moreover, in a supporting experimental approach, MXC was demonstrated to enhance the wound healing capacity of pHAKCs in a standard *in vitro* wound healing scratch assay as compared to $MgCl_2$, used as both an experimental and osmotic control (Fig. 2G&H). The biological process underpinning these observations are currently being investigated at a molecular level. However, the findings elucidated in these current studies highlight the regenerative and healing potential of MXC in the skin.

3.5. Real-time cellular analysis of primary human dermal fibroblasts in response to MXC

Complimentary studies were carried out, using Primary Human Normal Dermal Fibroblast Cells (Fig. 3). Experimental protocols were precisely the same (cell number, MXC concentrations, ECM compositions, xCELLigence® settings and running protocol). Initial observations over the 48 h were the cellular response, kinetics and dynamics of fibroblasts differed considerably from that of the keratinocytes. This highlights an important biological observation that there is a different cell specific response to MXC, emphasising the point that it elicits a precise response which depends on the particular cell profile (signalling networks, proteomic and transcriptomic compliment, receptor expression levels, e.g. TRPM7, MagT1 or integrins). Cell adhesion kinetics displayed a biphasic effect (0.1–1.5%) with Dermal Fibroblasts (data not shown), a previously reported cellular response [63,64], but at all concentration (0.1%–0.8%) cell adhesion dynamics (kinetics/rate and extent) was greater than control fibroblasts (Fig. 3). Initial adhesion was slow (0–1.3 h), but increased exponentially from 1.3 h to 1.6 h, with all concentrations of MXC having a potentiating effect- indicating a potential beneficial effect of wound healing and skin regeneration. Cell spreading dynamics (1.6 h–3 h) again displayed a potentiating effect of MXC on active cell spreading. Similar to the keratinocyte studies, this has implications for cellular architecture and rigidity (i.e. tensegrity, form and function of cytoskeletal architecture etc.), and thus biomechanical properties of skin (elasticity, tone, barrier) [1]. Again, in a supporting experimental approach, MXC was demonstrated to enhance the wound healing capacity of pNHDFCs in a standard *in vitro* wound healing scratch assay as compared to osmotic and experimental controls (Mg Aspartate) (Fig. 3C–E). Interestingly, the highest concentration of MXC (1.5%) demonstrated the most profound beneficial effect in this regard, followed by concentrations 0.2% and 0.4%. 0.8% MXC displayed a slightly reduced cell spreading. This reduction was over come after the 3-h time point, when all concentrations (bar the 0.6% and 0.8% - data not shown) displayed an increased cellular integrity within the ECM, and an improved cell proliferation profile. Overall, these experiments demonstrate that MXC has the potential to improve fibroblast cell health and dynamics, as well as improved wound healing capacity, and improve the biomechanical properties of the

skin. To further elucidate these potential biological effects, further cellular and molecular studies were undertaken.

3.6. Cellular analysis (RTCA, wound healing & angiogenesis tube formation) of primary human aortic endothelial cells in response to MXC

In order to facilitate regeneration of normal tissue in damaged areas, neovascularisation and collagen synthesis followed by re-epithelialisation are important processes of note [65,66]. Migration and proliferation are crucial steps in the highly complex and co-ordinated series of events that lead up to angiogenesis, where sprouts invade the newly ECM-rich wound and organise into a microvascular network throughout the granulation tissue. The process requires the activation of several signalling pathways converging on cytoskeletal remodelling [67]. Moreover, these processes are influenced by extra-cellular signals from the local microenvironment. Data show that MXC treatment demonstrated significantly greater ($P \leq 0.05$) levels of tube formation in comparison to Mg Aspartate control in HAECs (Fig. 5C&D). This is consistent with migration and wound healing data, (Fig. 5A&B). It was noted that $MgCl_2$ had a slightly more potent effect on HAEC migration in a monoculture *in vitro* wound healing scratch assay (Fig. 5A&B).

3.7. Cooling efficacy of dressing with visco-elastic gel and MXC (EBD + MXC)

In order to assess the cooling effect of EBD + MXC upon burn injury, an *in vitro* 3D organotypic human skin equivalent platform, LabSkin, was modified to facilitate thermal monitoring post burn injury (Fig. 5). To our knowledge, this is the first time a deep tissue, humanised living skin equivalent has been pioneered and utilised for the interrogation of the (patho-) physiology of burn injury, and the cellular and molecular mechanisms behind repair and regeneration. This adds to our current body of knowledge in effectively modelling human diseases *in vitro*, in order to obtain more relevant clinical data in an ethical, cost and time effective manner, thus accelerating burn and chronic wound research for societal and patient benefits [68]. Briefly, a custom-built 12 V thermostatically-controlled waterproof heating apparatus was engineered to simulate body temperature *in vitro* and assess the cooling effects of running water vs EBD + MXC post thermal insult. Injury was precisely delivered by custom-milled brass weights (3.66 g, 10 mm diameter), which were heated to 100 °C prior to application to the LabSkin model. Mean sub-dermal temperatures were monitored over time for each treatment group. Temperature of the 3D model during and after administration of a 15 s burn was measured every 10 s using a temperature probe placed at 4 mm depth below the skin surface. Time 0 = start of burn application. Results are averaged from three independent experiments \pm SD. The application of EBD + MXC had a cooling effect immediately upon application and levelled out to body temperature within 6–7 min post application. This was opposed to running water which cooled the burn injury to <30 °C within 120 s. However, this important difference may affect hypothermia in patients and have profound relevance to morbidity and mortality outcomes in an emergency setting

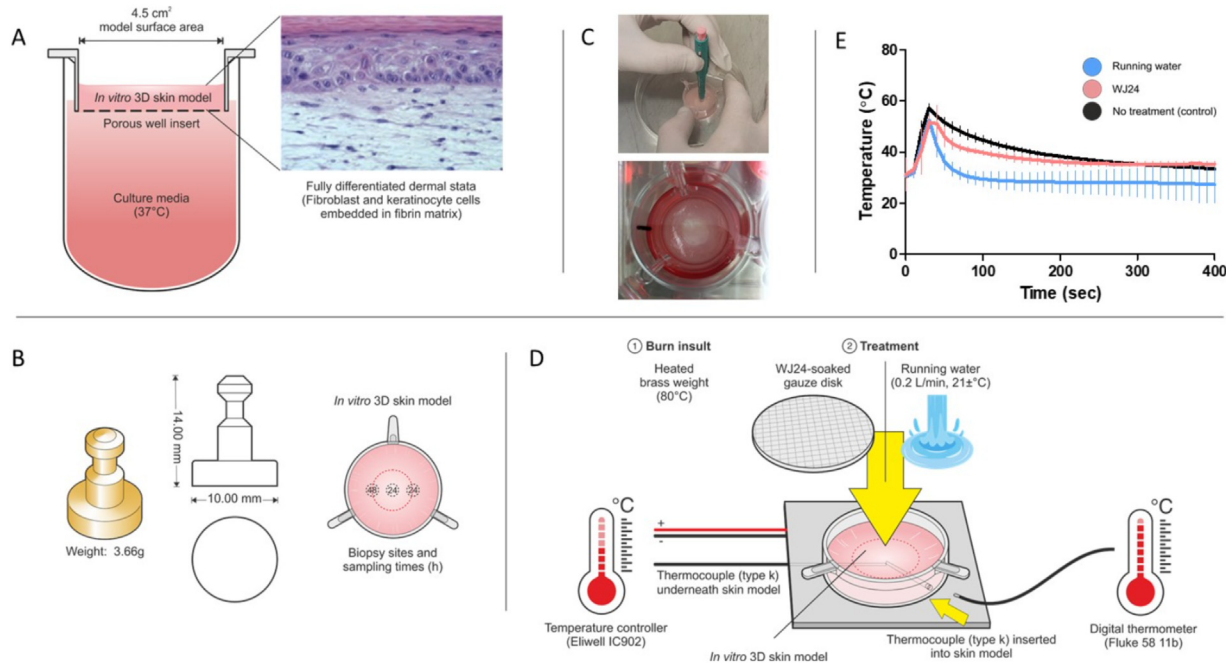


Fig. 5 – Establishment of 3D LabSkin™ model for burn studies. (A) Illustration of the 3D LabSkin™ model indicating differentiated dermal layers and culturing conditions. **(B)** Custom-milled brass weights were used to deliver the thermal insult. Burn radius (red line) and 24- and 48-h biopsy sites are indicated to the right. **(C)** Appearance immediately following burn: Model turned white in the centre following removal of the weight. All models were biopsied using a 3 mm biopsy punch (MilteX) in the centre and at the burn margin 24 h after the burn was inflicted, and conditioned media was sampled. **(D)** Custom-built 12 V thermostatically-controlled waterproof heating apparatus to simulate body temperature *in vitro* and assess effects of running water vs EBD + MXC **(E)** Cooling Effect of WJ24 treatment compared to running water. Mean sub-dermal temperatures over time for each treatment group. Temperature of the 3D model during and after administration of a 15 s burn was measured every 10 s using a temperature probe placed at 4 mm depth below the skin surface. Time 0 = start of burn application. Results are averaged from three independent experiments ± SD.

post-burn. This immediate cooling effect could be witnessed in the preservation of viable tissue, an observation assessed by qualitative and quantitative analysis of RNA from biopsies taken at time points post thermal injury Table 4 (Supplementary material). Treatment with EBD+MXC preserved viable tissue post burn injury.

3.8. Effect of MXC on gene expression on an *in vitro* monoculture of primary human dermal fibroblasts

In order to ascertain if MXC elicited its functional effect observed in Figs. 2–4 via modulation of gene expression, monocultures of primary human dermal cells were treated with two concentrations of MXC and RNA was harvested at 24 h post treatment along with no treatment and osmotic controls as gene expression references. Gene profiling demonstrated a molecular effect of MXC on primary human dermal cells, which may explain the functional effects observed during RTCA (*data not shown*). However, it must be noted that there was a high degree of overlap with the LabSkin transcriptomic data.

3.9. Temporal molecular validation of thermal insult model

In order to validate the LabSkin organotypic human skin equivalent model, biopsies were taken at two time points

from time of burn insult- 24 and 48 h post burn. For the purposes of this study only time point 24 h post burn will be presented. Current and future studies are investigating various temporal time points (0–72 h) using an integrated ‘-omics’ approach, together with data analytics and pathway analysis. No burn control biopsies were obtained at the relevant time points as comparative controls. RNA was isolated and a focused transcriptomic analysis was undertaken to survey 84 genes involved in the wound healing process. Fig. 6A–D illustrates that there was indeed a gene expression regulation upon injury and various treatment modalities at the 24-h time points, validating the burn effect on the 3D organotypic human skin equivalent model. Table 1 highlights the statistical relevant variations in wound healing gene expression with respect to 24-h post-burn upon treatment with EBD-MXC.

3.10. Wound healing and fibrosis analysis of EBD ± MXC application to burn injury versus (i) no burn and (ii) burn control employing focused pathway gene arrays (Qiagen RT² profiler arrays) and *in vitro* LabSkin burn model

A comprehensive molecular profiling study was undertaken to assess the effect of EBD ± MXC on burns using the *in vitro* LabSkin organotypic human skin equivalent model (Figs. 6,7).

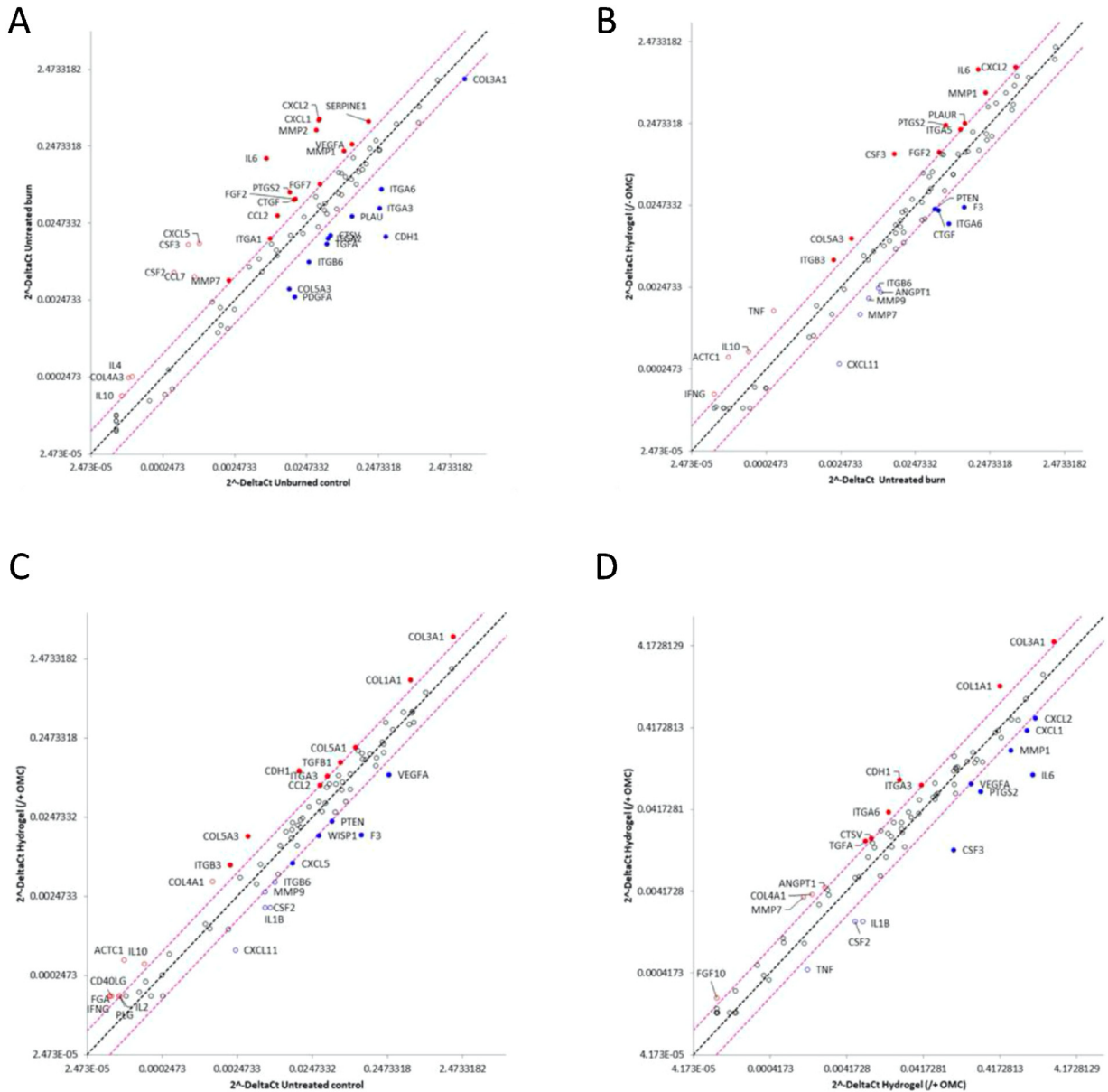


Fig. 6 – Molecular wound healing response to thermal insult 24 h post burn (B24hr) upon EBD treatment with and without MCX (EBD ± MXC), compared to B24hr no treatment control (NTC). Effect of EBD ± MXC v burn on wound healing mRNA expression 24 h post-burn. (A) Untreated burn v unburned control. (B) EBD-MXC v untreated burn. (C) EBD + MXC v untreated burn. (D) EBD + MXC v EBD-MXC. Scatter plot represents normalised gene expression for all genes present on the array. The central line indicates unchanged gene expression. Dotted lines indicate selected fold regulation threshold. Data points beyond these represent genes that meet the selected 2-fold regulation threshold. Appropriate corrections were made using proprietary Qiagen RT2 analysis software. CT cut-off was set at 35. CT values for endogenous control genes were geometrically averaged and used in ΔΔCT calculations. (n = 3 for each array).

The cooling effect alone versus cooling and pro-healing/anti-fibrotic (MXC) effect (Fig. 6B-D & Fig. 7B-D)) was also investigated using focused pathway gene arrays (Qiagen RT² profiler arrays). Experimental attention was given to the 24 h post-burn time point (B24hr) upon treatment with EBD ± MXC versus No Burn Control (NBC24hr), as the EBD was developed with the goal of cooling thermal injury, preserving tissue, initiating the healing process and ameliorate scar formation

within the first 24 h of burn injury. Moreover, subsequent to this analysis we undertook a 48 h study to assess the prolonged and sustained effect of EBD ± MXC on burned skin. Attention was also given to the fibrosis gene expression profile at both the 24 h and 48 h time points with applied EBD ± MXC, as chronic perturbations to the healing process can result in pathological scar formation. The cooling effect alone (EBD - MXC) on burn injury up-regulated 14 genes and

down-regulated 9 genes involved in the wound healing process. EBD + MXC further up-regulated 11 genes and down-regulated 10 genes involved in the wound healing process, emphasising the initiation of the healing process in the first 24 h post burn upon application of EBD + MXC (Table 1). This phenomenon is in addition to the cooling/tissue preservation effect of EBD + MXC on burn injury.

The cooling effect alone (EBD - MXC) on burn injury up-regulated 14 genes and down-regulated 9 genes involved in the wound healing process. EBD + MXC further up-regulated 11 genes and further down-regulated 10 genes involved in the wound healing process, emphasising the initiation of the healing process in the first 24 h post burn upon application of EBD + MXC. This phenomenon is in addition to the cooling/tissue preservation effect of EBD - MXC on burn injury. At the 48 h time point, the cooling effect alone (EBD - MXC) on burn injury up-regulated 14 genes and down-regulated 27 genes involved in the wound healing process. Further to this molecular effect of EBD cooling capacity, an additional 12 genes were up-regulated and 10 genes down-regulated upon EBD + MXC treatment at the 48-h time point (*data not shown*).

To assess the anti-fibrotic effect of EBD + MXC, parallel studies were undertaken employing the Qiagen RT² Fibrosis profiler array to interrogate 84 genes directly involved in scarring. Similar beneficial transcriptomic changes beneficial were observed at both time points, with cooling alone (EBD - MXC) modulating 10 (up) and 8 (down) genes at the 24-h time point. The additive effect of MXC was observed with the additional modulation of 5 (up) and 9 (down) genes at the 24-h time point (Fig. 7A–D & Table 1). The cooling effect of the EBD elicited an up-regulation of 14 genes and down-regulation of a further 26 at the 48 h time point (*data not shown*). This potential anti-scarring effect was augmented by the addition of MXC (EBD + MXC), with an additional 10 genes up-regulated and 12 genes down-regulated to those observed with cooling alone (EBD - MXC).

4. Discussion

“Healing is not a science, but the intuitive art of wooing nature.”
Wystan H. Auden.

The field of wound and burn repair continues to grow at an astonishing rate. Notwithstanding the major strides in the advancement of therapeutic strategies for burns treatment and care over the recent number of decades, skin burns from multiple sources exert catastrophic influences on human morbidity and mortality [6,24,28]. Herein, we report the development of a novel thermal burn model, employing a humanised *in vitro* living deep-skin equivalent, LabSkin[®]. This facilitated the real-time measurements of temperature fluctuations pre-and post-burn insult, as well as monitoring cooling effects of standard running water versus a novel composite visco-elastic gel (EBD + MXC). Furthermore, this *in vitro* approach allowed molecular interrogation of both burn healing and fibrosis cellular mechanisms. LabSkin is an *in vitro* model and as such cannot completely recapitulate the whole physiological response of the real human body. The current

Table 1 – The Effect of Untreated Burn Injury versus Treated Burn Injury on both Wound Healing & Fibrosis mRNA expression in a 3D LabSkin living human dermal model, 24 h post-burn (n = 3). Note that data shown are a selected representation of total differentially expressed genes and are limited to fold changes of 2 or above. All displayed data demonstrated a statistical significance of $P < 0.005$. Duplicated genes between both focused pathway RT² Profiler PCR Arrays were accounted for and only one result presented for clarity of table presentation.

24 h post burn injury			
Treatment versus untreated			
Wound healing		Fibrosis/scarring	
Gene	Fold change	Gene	Fold change
CSF3	8.01	CXCR4	11.36
IL6	6.51	CCL3	10.50
CDH1	5.76	CCR2	6.99
ACTC1	5.13	ITGB3	4.22
COL5A3	4.12	BCL2	3.83
PTGS2	3.74	TNF	3.55
COL4A1	3.26	IL10	3.35
FGA	2.76	MMP13	3.29
IFNG	2.76	PLG	2.80
MMP1	2.73	MMP1	2.75
ITGB3	2.69	TGFB3	2.69
COL1A1	2.66	ENG	2.49
CD40LG	2.59	IFNG	2.33
COL3A1	2.54	MYC	2.31
CXCL2	2.26	COL3A1	2.21
PLAUR	2.16	TGFB3	2.20
FGF2	2.16	PDGFA	2.05
ITGA3	2.11	SMAD7	2.05
TGFB1	2.10	TGFB2	-2.01
ITGA5	2.08	EDN1	-2.03
PLG	2.05	IL1B	-2.25
IL2	2.04	ITGA1	-2.26
COL5A1	2.03	IL1A	-2.28
CCL2	2.00	CTGF	-2.29
WISP1	-2.07	IL13RA2	-2.30
PTEN	-2.07	MMP3	-2.33
CXCL5	-2.08	SERPINA1	-2.73
CTGF	-2.30	MMP9	-2.85
CSF2	-3.20	VEGFA	-3.06
MMP9	-3.22	GREM1	-3.11
IL1B	-3.75	ITGB6	-3.40
MMP7	-3.88	IL1A	-3.90
ANGPT1	-3.97	EDN1	-4.78
ITGA6	-4.64	CCL11	-5.53
F3	-7.63		

LabSkin model lacks vasculature (currently in development) which implies that parts of the healing response, such as infiltration of granulocytes, macrophages and lymphocytes, are absent. However, LabSkin healing occurs, similar to *in vivo* human skin, by re-epithelialisation [69], expressing, during this process, genes related to cell growth, cell differentiation and tissue remodelling. In contrast, some animal models used for the study of the healing process display a healing mechanism driven by contraction.

Although, it is true that the LabSkin model lacks immunocompetent and Langerhans cells, it is well known that Keratinocytes express TLR1-6 and -9 [70] and that this is

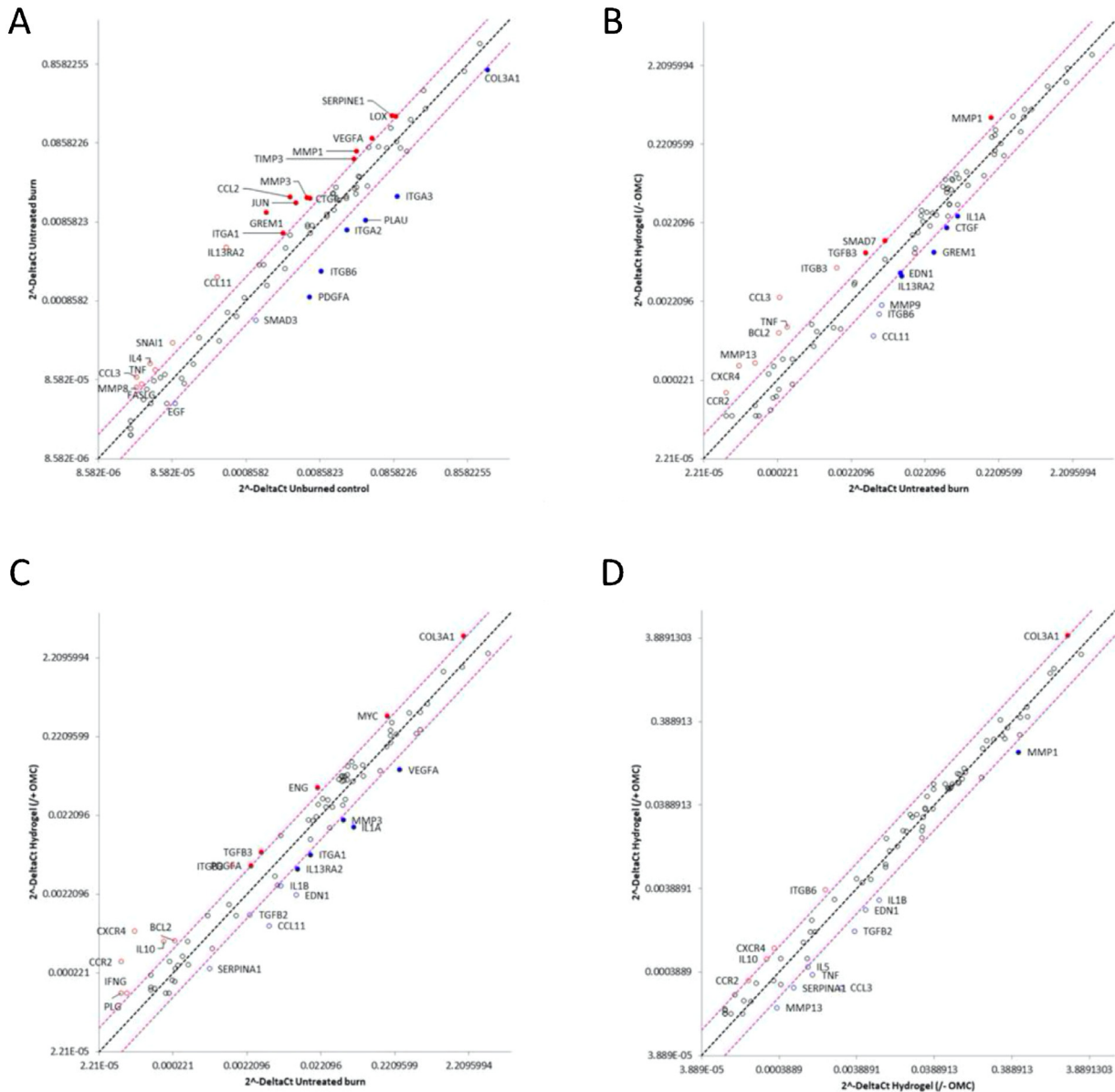


Fig. 7 – Molecular fibrosis/scar response to thermal insult 24 h post burn (B24hr) upon EBD treatment with and without MXC (EBD ± MXC), compared to B24hr no treatment control (NTC). Effect of EBD ± MXC v burn on fibrosis mRNA expression 24 h post-burn. (A) Untreated burn v unburned control. (B) EBD-MXC v untreated burn. (C) EBD + MXC v untreated burn. (D) EBD + MXC v EBD-MXC. Scatter plot represents normalised gene expression for all genes present on the array. The central line indicates unchanged gene expression. Dotted lines indicate selected fold regulation threshold. Data points beyond these represent genes that meet the selected 2-fold regulation threshold. Appropriate corrections were made using proprietary Qiagen RT2 analysis software. CT cut-off was set at 35. CT values for endogenous control genes were geometrically averaged and used in $\Delta\Delta$ CT calculations. (n = 3 for each array).

important in the response against pathogenic microorganisms. For instance, activation of TLR2 by *S. aureus* results in activation of NF- κ B a subsequent production of chemokine IL-8 that attract neutrophils (IL-8 is absent in mice, although some functional homologues have been suggested).

The LabSkin model specifically respond to pathogens such as *S. aureus* [71] by release of IL-23 and IL-8. Additionally, we have unpublished data showing the response of LabSkin to several insults such infection by bacteria (*S. aureus*, *E. coli*) and fungi (*C. albicans*, *Dermatophytes*, *Malassezia* spp.): uncolonised

wounds and wounds colonised with bacteria, fungi, and inter-kingdom polymicrobial biofilms; and chemical insults (unpublished data). LabSkin responds by releasing several signalling molecules: IL-1 α , IL-1 β , IL-6, IL-8, TNF- α , PTGS2 (indicative of prostaglandin production). Furthermore, LabSkin keratinocytes produce antimicrobial peptides RNase-7, which does not have a clear orthologue in mice [72], LL-37, which orthologue in murine models has different activity [73] and several defensins such as HBD-2. Fibroblast are also known to express TLR1-10 [74]. Data obtained from this

dynamic human *in vitro* 3D-organotypic burn model, were supported by cell fate and function assays using Real-Time Cellular Analysis (RTCA xCELLigence). Components of the EBD + MXC were assessed for their efficacy in modulating cellular tensegrity, adhesion, spreading and migration which are biologically integral for the burn healing process. To further support the observed healing capacity of MXC component, angiogenesis studies were undertaken, again a crucial phase for the reparative process of burn healing and dependent on endothelial cell migration.

In austere or mass casualty situations, where resources and level of care are limited, efficient and effective primary care within the first 24 h, prior to admission to a specialist burn centre or intensive care unit, is crucial. During this time frame, the goal of any primary treatment is to stop the burning process in order to preserve vital tissue viability and integrity as well as preventing subsequent loss through necrosis, thereby minimising the Zone of Coagulation and maximising the Zone of Stasis. Herein, we report the ability of the EBD + MXC to rapidly cool the thermal injury comparable to the standard of running water. Moreover, we observed a much greater RNA integrity levels RINe value (RINe = RNA integrity number- data in Table 4 of Supplementary material) in biopsy samples obtained from EBD + MXC treated burns as opposed to untreated. This is directly indicative of viable tissue being preserved and an inhibition of burn conversion. As the extent of cooling does not drop below body temperature, the possibility of post-burn hypothermia is minimised in contrast to application of running water. Moreover, as EBD + MXC is sterile and conforms to the injured area, introduction of microbial infection is minimised as the wound is protected. Microcidal assessment of EBD + MXC also demonstrated the bactericidal properties of the dressing. Antimicrobial activity is primarily through the action of the impregnated polymer, polyhexamethylene biguanide (PHMB), which kills bacteria selectively over host cells by entering bacteria and selectively condensing bacterial chromosomes [75]. Given the grave consequences of antibiotic resistant bacterial infection and sepsis, especially in the burn setting, the development of novel therapeutic approaches is a matter of urgency. It has been demonstrated that calcium and magnesium ions (Ca^{2+} and Mg^{2+}), the principle components of MXC, both disrupt model *S. aureus* membranes and kill stationary-phase *S. aureus* cells, indicative of membrane-activity [76]. The properties of the MXC copper ions are also biocidal, and the Ca^{2+} simulates and supports initial front-line immune surveillance [77–79].

The beneficial biophysical properties of EBD + MXC demonstrated, *i.e.* cooling, protection, and microbicidal were further supported by both *in vivo* and *in vitro* hydration studies. Maintaining a hydrated wound environment is pivotal in the repair and regeneration responses to burn injury. Tissue Dielectric Constant analysis using *in vitro* LabSkin treated with EBD with or without MXC demonstrated the improved hydration up to 24 h with EBD + MXC as opposed to EBD-MXC, highlighting the properties of MXC and confirmed the improvement of skin barrier formation with MXC treatment. *In vivo* analysis, while highlighting the inter individual responses observed due to environmental and biological architecture, supported the *in vitro* findings. Monoculture experiments using RTCA further consolidated these results and barrier

forming properties of MXC. Thus, in addition to halting the burning process, while providing a cooling and hydrating environment for the burn wound and simultaneously relieving pain and avoiding hypothermia, EBD + MXC also met important criteria such as a) providing an effective barrier to infective agents such as bacteria while providing an anti-microbial environment for the damaged area, thus preventing a *nidus*, b) has optimal physical properties such as drapeability/landscape conforming, elasticity, non-adherent and be semi-permeable to oxygen and water, and c) is hypoallergenic, biocompatible, non-inflammatory, anti-inflammatory and non-immunogenic.

To augment these crucial properties we sought to immediately provide and stimulate a healthy healing and regenerative capacity, two distinct but non-mutually exclusive biological processes, to the burn area before specialist care and intervention, thus improving patient outcomes. While efficient healing of skin wounds is crucial for securing the vital barrier function of the skin, pathological wound healing, fibrosis and scar formation are major medical problems causing both physiological and psychological challenges for patients. To further our knowledge and understanding, we employed a unique, integrated, multiple technological approach to comprehensively demonstrate the beneficial properties of this novel EBD + MXC to initiate and temporospatial support burn repair and regeneration. A number of tightly coordinated temporospatial regenerative responses, including haemostasis, the migration and proliferation of various cell types into the wound, inflammation, angiogenesis, and extracellular matrix turnover, are involved in this healing process. These cellular events require the highly regulated and finely orchestrated interplay among various dermal cell types, soluble factors and the extracellular matrix.

For optimal healing and regeneration, the wound microenvironment must meet a set of criteria to support and be specific to regeneration. On this basis, a proprietary Marine Mineral Complex (MXC) was developed and tested. MXC is concentrated in magnesium, potassium, sodium and boron at the molar ratio of 130:27:27:1 (Table 5. Certificate of Analysis in Supplementary material), in addition to containing trace levels of calcium, copper, silicon and zinc. Trace minerals (TM) are known to play a role in maintaining the structural integrity of different tissues including skin [48,80–82], and promote a healing, regenerative environment [47,48,83]. It is well recognised that Mg^{2+} and Ca^{2+} are *conditio sine qua non* for wound healing, regulating both cell signalling and gene expression. This in turn, regulates the production and maintenance of ECMs *e.g.* collagen and proteoglycans (GAGs), regulation of matrix metalloproteinases (MMPs) activity, cell proliferation and migration [84,85].

In order to fully assess the effect of MXC on dermal cell adhesion, spreading, migration and proliferation, we employed Real Time Cellular Analysis of primary human dermal a) fibroblasts b) keratinocytes and microvascular endothelial cells. As cellular response is measured in real time, as opposed to end point assays, we were able to monitor cellular healing kinetics, *i.e.* rate, as well as the extent of cell adhesion, spreading, migration and proliferation. It was found that the appropriate concentrations of MXC indeed did stimulate and support these cellular functions intrinsic to wound healing.

Having assessed the cellular responses to MCX, focused gene transcriptomic studies were utilised to elucidate the molecular basis to the observed cellular functions. To this end, two focused arrays were employed, wound healing and fibrosis, to ascertain the molecular effect of EBD + MXC and EBD-MXC on burn injury both at 24 h and 48 h post thermal insult on a LabSkin model. Burned but untreated and non-burned were used as comparative experimental controls. As expected the cooling effect of the EBD (without MXC) alone had a beneficial effect on gene expression, as tissue was preserved and protected post application of EBD. This effect was further enhanced by cooling with MXC present, i.e. EBD + MXC. The comparative gene expression profiles of unburned control *versus* burned-untreated control demonstrated the validity of the LabSkin platform for burn studies. When assessing the effect of EBD + MXC treated burn *versus* untreated control burn on wound healing mRNA expression at 24 h post-burn ($n = 3$), it was found that in total, 17 genes were up-regulated within a >2 -fold limit in response to EBD + MXC treatment in comparison to an untreated burn control. These included the anti-inflammatory cytokine, IL10, and importantly a number of ECM-producing genes (COL5A3, COL4A1, COL1A1, COL3A1, COL5A1) in addition to inflammatory marker, IL2. 10 genes were down-regulated, consisting of integrins, MMPs and the pro-angiogenic gene, VEGFA.

In parallel and in conjunction to the wound healing array, we also employed and interrogated a fibrosis array. When assessing the effect of EBD + MXC treated burn *versus* untreated control burn on genes involved in fibrosis, 24 h post-burn ($n = 3$), 12 genes exhibited up-regulation within the >2 -fold limit in comparison to the untreated control. These included ITGB3, COL3A1, ENG and PDGFA. In response to the same treatment, 10 genes demonstrated down-regulation. These included a number of integrins, interleukins and VEGFA. Importantly, a serendipitous discovery of a 3 fold reduction in both colony-stimulating factor 2 and VEGFA was discovered. CSF2 and VEGFA are both pivotally involved in heterotopic ossification (HO), a frequent complication of modern wartime extremity injuries [86,87].

While transcriptomic array data is insightful at a holistic level, the three dimensional interplay between these genes and gene products determine the wound healing capacity and anti-fibrotic potential of EBD + MXC. These comparative gene expression studies supported RTCA data on the effect of MXC on dermal cellular function. Future work to include bioinformatic and pathway analysis will establish the interplay between these gene networks and signalling hubs such as cellular pathway analysis and microRNA expression [88], allowing us to gain further insight into ‘the gentle wooing’ of the reparative and regenerative process for burns and chronic wounds.

5. Conclusion

This study advances our in depth understanding of the biomaterial/wound environment interplay. This has led to the development of a novel solution to overcome current limitations in burn treatments, which still represent an important challenge in the biomedical field. This composite

visco-elastic dressing with integrated multi-functionality, stimulated by the proprietary MXC represents a new therapeutic strategy to overcome current clinical challenges in the treatment of injuries resulting from burns. It is biocompatible and hypoallergenic, protective, non-adherent, hydrating, and cooling. MXC as a bio-stimulatory conditioning agent which is readily and rapidly bio-absorbable. It combines the optimal physiological and physical dressing properties together for use in both adults and children, in a primary/emergency care setting, reducing the frequency of subsequent dressing changes allowing for use in prolonged care. Thus, we believe that this hybrid emergency burn dressing (EBD + MXC) can be widely applied and used in a primary care and pre-surgical settings for the treatment of burns with optimal therapeutic effect.

Author contributions

B.D., G.M., N.M.M., M-A.C., a.m., R.p.m. contributed to the conception and design of the work; R.G.W., M-R.K, A.J.B., L.T., E.D., B.D., M-A.C., a.m., R.p.m. contributed to the acquisition, analysis, or interpretation of data for the work; B.D., D.C-L., N.M.M., G.M., M-A.C., R.p.m. contributed to the drafting of the paper and in revising it critically for important intellectual content; and all authors approved the final version to be published.

Disclosure of interest statement

R.p.m. acknowledges the funding support of Science Foundation Ireland (SFI Technology Innovation Development Award-11/TIDA/B1927), the Innovation Partnership Program which is co-funded by Enterprise Ireland and the European Regional Development Fund (ERDF) under Ireland’s European Structural and Investment Funds programmes, EI Industrial Research and Commercialisation Committee (PC-2009-0311, INV/13000/001/2015, IP 2015 0399Y, IP 2015 0418 & IP 2017 0587). R.G.W. & L.T. were in part supported by an Irish Research Council for Science, Engineering & Technology (IRCSET) EMBARK Post-graduate Scholarship 2011–2014 (RS/2011/695 & RS/2012/2499) and R.G.W., A.J.B. and M-R.K. through funding awarded to R.p.m. from EI and Oriel Sea Salt (2015–2019). RPM is a management committee member of the EU H2020 COST actions- CM1406 & CA18127. In the interest of full disclosure, Oriel Sea Salt is the manufacturer and supplier of the marine ingredient necessary for the research (MXC). Oriel Sea Salt co-funded the research (30%) as required under Irish Government state funding rules, with grants of 70% received from Irish Government Agencies, EI and SFI, in accordance with the agencies IRCC regulations, and to the EU Horizon 2020 Responsible Research & Innovation principals. The authors acknowledge that Oriel Sea Salt have potential commercial interest in the outputs from this research and hold various patents in relation to the production, purification and use of MXC. R.p.m. was awarded an honorarium from BioMed Central/Springer Nature (2020), and serves on the Board of Directors for the charity My Canine Companion. In addition, R.p.m. (1) has received research industry funding from Neal’s Yard

Remedies, Bord Iascaigh Mhara and BiaNutra Ltd., (2) scientifically consulted for Neal's Yard Remedies, WhiteSwell, Shire Pharmaceuticals, and Java Clinical Research and (3) has spoken at meetings and symposia sponsored by various food, pharmaceutical, cosmetic and medical device & diagnostic companies. All other authors report no financial, professional or personal conflicts of interest relating to this publication. In accordance with the Community Framework For State Aid For Research and Development and Innovation (2006/C 323/01) as implemented by EI, the outputs of this Research are owned by DCU. Dr. David Caballero-Lima is an employee of LabSkin.

Acknowledgements

We wish to acknowledge Liam Meany, Simon Morgan, David Mothersole & Dr. Hodger Wedler for their technical assistance, critique and advice. We would also like to thank Mr. Brian Fitzpatrick and Dr. Jordan K. Magtaan for serving as advisors, critically reviewing the study proposal and participated in the technical editing of the manuscript. As part of this study, we would like to thank Oriel Marine Research (Ire), LabSkin (Ire) and WaterJel Technologies, (USA) who kindly contributed materials and relative supportive data and input as required to complete the study.

Appendix A. Supplementary data

Supplementary material related to this article can be found, in the online version, at doi:<https://doi.org/10.1016/j.burns.2020.04.036>.

REFERENCES

- [1] Ingber DE. From mechanobiology to developmentally inspired engineering. *Philos Trans R Soc Lond B Biol Sci* 2018;373(1759).
- [2] Trustees ABABO, Care CoO, Delivery of B. Disaster management and the ABA plan. *J Burn Care Rehabil* 2005;26(2):102–6.
- [3] Al-Benna S. Adequate specialised burn care services are essential at major trauma centres. *Burns* 2013;39(7):1495–7.
- [4] Pham C, Greenwood John, Cleland Heather, Woodruff Peter, Maddern Guy. Bioengineered skin substitutes for the management of burns: a systematic review. *Burns* 2007;33(8):946–57.
- [5] Clark A, Neyra JA, Madni T, Imran J, Phelan H, Arnoldo B, et al. Acute kidney injury after burn. *Burns* 2017;43(5):898–908.
- [6] Crowe CS, Massenburg BB, Morrison SD, Naghavi M, Pham TN, Gibran NS. Trends of burn injury in the United States: 1990 to 2016. *Ann Surg* 2019;270(6):944–53.
- [7] Pham C, Collier Z, Gillenwater J. Changing the way we think about burn size estimation. *J Burn Care Res* 2019;40(1):1–11.
- [8] Barillo DJ, Wolf S. Planning for burn disasters: lessons learned from one hundred years of history. *J Burn Care Res* 2006;27(5):622–34.
- [9] Smolle C, Cambiaso-Daniel J, Forbes AA, Wurzer P, Hundeshagen G, Branski LK, et al. Recent trends in burn epidemiology worldwide: a systematic review. *Burns* 2017;43(2):249–57.
- [10] Allison K, Porter K. Consensus on the pre-hospital approach to burns patient management. *Injury* 2004;35(8):734–8.
- [11] Roth JJ, Hughes W. The essential burn unit handbook, Second edition. Second edition .
- [12] Ainsworth CR, Dellavolpe J, Chung KK, Cancio LC, Mason P. Revisiting extracorporeal membrane oxygenation for ARDS in burns: a case series and review of the literature. *Burns* 2018;44(6):1433–8.
- [13] Yurt RW, Bessey PQ, Bauer GJ, Dembicki R, Laznick H, Alden N, et al. A regional burn center's response to a disaster: September 11, 2001, and the days beyond. *J Burn Care Rehabil* 2005;26(2):117–24.
- [14] Mason SA, Nathens AB, Byrne JP, Fowler RA, Karanicolas PJ, Moineddin R, et al. Burn center care reduces acute health care utilization after discharge: a population-based analysis of 1,895 survivors of major burn injury. *Surgery* 2017;162(4):891–900.
- [15] Ogunbileje JO, Herndon DN, Murton AJ, Porter C. The role of mitochondrial stress in muscle wasting following severe burn trauma. *J Burn Care Res* 2018;39(1):100–8.
- [16] Kennedy PJ, Haertsch PA, Maitz PK. The Bali burn disaster: implications and lessons learned. *J Burn Care Rehabil* 2005;26(2):125–31.
- [17] Renz EM, King BT, Chung KK, White CE, Lundy JB, Laird KF, et al. The US Army burn center: professional service during 10 years of war. *J Trauma Acute Care Surg* 2012;73(6 Suppl. 5):S409–16.
- [18] Cancio LC, Horvath EE, Barillo DJ, Kopchinski BJ, Charter KR, Montalvo AE, et al. Burn support for Operation Iraqi Freedom and related operations, 2003 to 2004. *J Burn Care Rehabil* 2005;26(2):151–61.
- [19] Gutierrez de Ceballos JP, Turégano Fuentes F, Perez Diaz D, Sanz Sanchez M, Martin Llorente C, Guerrero Sanz JE. Casualties treated at the closest hospital in the Madrid, March 11, terrorist bombings. *Crit Care Med* 2005;33(1 Suppl):S107–12.
- [20] Sheffy N, Mintz Y, Rivkind AI, Shapira SC. Terror-related injuries: a comparison of gunshot wounds versus secondary-fragments-induced injuries from explosives. *J Am Coll Surg* 2006;203(3):297–303.
- [21] Wolf SE, Kauvar DS, Wade CE, Cancio LC, Renz EP, Horvath EE, et al. Comparison between civilian burns and combat burns from Operation Iraqi Freedom and Operation Enduring Freedom. *Ann Surg* 2006;243(6):786–92 discussion 92–95.
- [22] Amaefule KE, Dahiru IL, Sule UM, Ejagwulu FS, Maitama MI, Ibrahim A. Trauma intensive care in a terror-ravaged, resource-constrained setting: are we prepared for the emerging challenge? *Afr J Emerg Med* 2019;9(Suppl):S32–7.
- [23] Mahoney EJ, Harrington DT, Biffi WL, Metzger J, Oka T, Cioffi WG, et al. Lessons learned from a nightclub fire: institutional disaster preparedness. *J Trauma* 2005;58(3):487–91.
- [24] Bloemasma GC, Dokter J, Boxma H, Oen IM. Mortality and causes of death in a burn centre. *Burns* 2008;34(8):1103–7.
- [25] Lundy JB, Swift CB, McFarland CC, Mahoney P, Perkins RM, Holcomb JB. A descriptive analysis of patients admitted to the intensive care unit of the 10th Combat Support Hospital deployed in Ibn Sina, Baghdad, Iraq, from October 19, 2005, to October 19, 2006. *J Intensive Care Med* 2010;25(3):156–62.
- [26] Potin M, Sénéchaud C, Carsin H, Fauville JP, Fortin JL, Kuenzi W, et al. Mass casualty incidents with multiple burn victims: rationale for a Swiss burn plan. *Burns* 2010;36(6):741–50.
- [27] Jeschke MG, Herndon DN. Burns in children: standard and new treatments. *Lancet* 2014;383(9923):1168–78.
- [28] Tsurumi A, Que YA, Yan S, Tompkins RG, Rahme LG, Ryan CM. Do standard burn mortality formulae work on a population of severely burned children and adults? *Burns* 2015;41(5):935–45.
- [29] Cambiaso-Daniel J, Rontoyanni VG, Focerrada G, Nguyen A, Capek KD, Wurzer P, et al. Correlation between invasive and noninvasive blood pressure measurements in severely burned children. *Burns* 2018;44(7):1787–91.

- [30] Cheng W, Shen C, Zhao D, Zhang H, Tu J, Yuan Z, et al. The epidemiology and prognosis of patients with massive burns: a multicenter study of 2483 cases. *Burns* 2019;45(3):705–16.
- [31] Liu NT, Rizzo JA, Shingleton SK, Fenrich CA, Serio-Melvin ML, Christy RJ, et al. Relationship between burn wound location and outcomes in severely burned patients: more than meets the size. *J Burn Care Res* 2019;40(5):558–65.
- [32] Christiaens W, Van de Walle E, Devresse S, Van Halewyck D, Benahmed N, Paulus D, et al. The view of severely burned patients and healthcare professionals on the blind spots in the aftercare process: a qualitative study. *BMC Health Serv Res* 2015;15:302.
- [33] Abdel-Sayed P, Hirt-Burri N, de Buys Roessingh A, Raffoul W, Applegate LA. Evolution of biological bandages as first cover for burn patients. *Adv Wound Care (New Rochelle)* 2019;8(11):555–64.
- [34] Lucas C, Baudry M, Chaouat M, Gachie L, Lefort H. Adult thermal burn dressings in three acts. *Rev Infirm* 2019;68(256):30–1.
- [35] Nour S, Baheiraei N, Imani R, Khodaei M, Alizadeh A, Rabiee N, et al. A review of accelerated wound healing approaches: biomaterial-assisted tissue remodeling. *J Mater Sci Mater Med* 2019;30(10):120.
- [36] Pan ZP, Han B, Chen XQ, Zhao YQ, Qin DY, Pang N, et al. Advances in the research of smart dressings. *Zhonghua Shao Shang Za Zhi* 2019;35(7):552–6.
- [37] Ribeiro DML, Carvalho Júnior AR, Vale de Macedo GHR, Chagas VL, Silva LDS, Cutrim BDS, et al. Polysaccharide-based formulations for healing of skin-related wound infections: lessons from animal models and clinical trials. *Biomolecules* 2019;10(1).
- [38] Walboomers XF, Jansen JA, Wagener FADT. Design considerations for hydrogel wound dressings; strategic and molecular advances. *Tissue Eng B Rev* 2020, doi:<http://dx.doi.org/10.1089/ten.teb.2019.0281> [Accessed 28 February 2020]. In press.
- [39] Abdel-Sayed P, Michetti M, Scaletta C, Flahaut M, Hirt-Burri N, de Buys Roessingh A, et al. Cell therapies for skin regeneration: an overview of 40 years of experience in burn units. *Swiss Med Wkly* 2019;149:w20079.
- [40] Hicks KE, Huynh MN, Jeschke M, Malic C. Dermal regenerative matrix use in burn patients: a systematic review. *J Plast Reconstr Aesthet Surg* 2019;72(11):1741–51.
- [41] El Hosary R, El-Mancy SMS, El Deeb KS, Eid HH, El Tantawy ME, Shams MM, et al. Efficient wound healing composite hydrogel using Egyptian *Avena sativa* L. Polysaccharide containing β -glucan. *Int J Biol Macromol* 2020;149(April):1331–8, doi: <http://dx.doi.org/10.1016/j.ijbiomac.2019.11.046>.
- [42] Esposito D, Overall J, Grace MH, Komarnytsky S, Lila MA. Alaskan berry extracts promote dermal wound repair through modulation of bioenergetics and integrin signaling. *Front Pharmacol* 2019;10:1058.
- [43] Matica MA, Aachmann FL, Tøndervik A, Sletta H, Ostafe V. Chitosan as a wound dressing starting material: antimicrobial properties and mode of action. *Int J Mol Sci* 2019;20(23).
- [44] Rezaei M, Oryan S, Javeri A. Curcumin nanoparticles incorporated collagen-chitosan scaffold promotes cutaneous wound healing through regulation of TGF- β 1/Smad7 gene expression. *Mater Sci Eng C Mater Biol Appl* 2019;98:347–57.
- [45] Zhang T, Liu F, Tian W. Advance of new dressings for promoting skin wound healing. *Sheng Wu Yi Xue Gong Cheng Xue Za Zhi* 2019;36(6):1055–9.
- [46] Medlin S. Nutrition for wound healing. *Br J Nurs* 2012;21(12):S11–2, S14–5.
- [47] Chen J, Tellez G, Escobar J, Vazquez-Anon M. Impact of trace minerals on wound healing of footpad dermatitis in broilers. *Sci Rep* 2017;7(1):1894.
- [48] Chen LR, Yang BS, Chang CN, Yu CM, Chen KH. Additional vitamin and mineral support for patients with severe burns: a nationwide experience from a catastrophic color-dust explosion event in Taiwan. *Nutrients* 2018;10(11).
- [49] Cantore S, Ballini A, Saini R, Altini V, De Vito D, Pettini F, et al. Effects of sea salt rinses on subjects undergone to oral surgery: a single blinded randomized controlled trial. *Clin Ter* 2020;170(1):e46–52.
- [50] Castillo-Briceno P, Bihan D, Nilges M, Hamaia S, Meseguer J, Garcia-Ayala A, et al. A role for specific collagen motifs during wound healing and inflammatory response of fibroblasts in the teleost fish gilthead seabream. *Mol Immunol* 2011;48(6–7):826–34.
- [51] Tassi E, McDonnell K, Gibby KA, Tilan JU, Kim SE, Kodack DP, et al. Impact of fibroblast growth factor-binding protein-1 expression on angiogenesis and wound healing. *Am J Pathol* 2011;179(5):2220–32.
- [52] Syed F, Bayat A. Notch signaling pathway in keloid disease: enhanced fibroblast activity in a Jagged-1 peptide-dependent manner in lesional vs. extralesional fibroblasts. *Wound Repair Regen* 2012;20(5):688–706.
- [53] Sherwood CL, Lantz RC, Boitano S. Chronic arsenic exposure in nanomolar concentrations compromises wound response and intercellular signaling in airway epithelial cells. *Toxicol Sci* 2013;132(1):222–34.
- [54] Kim KH, Chung WS, Kim Y, Kim KS, Lee IS, Park JY, et al. Transcriptomic analysis reveals wound healing of *Morus alba* root extract by up-regulating keratin filament and CXCL12/CXCR4 signaling. *Phytother Res* 2015;29(8):1251–8.
- [55] Fox SJ, Fazil MH, Dhand C, Venkatesh M, Goh ET, Harini S, et al. Insight into membrane selectivity of linear and branched polyethylenimines and their potential as biocides for advanced wound dressings. *Acta Biomater* 2016;37:155–64.
- [56] Duffy E, Guzman KD, Wallace R, Murphy R, Morrin A. Non-invasive assessment of skin barrier properties: investigating emerging tools for in vitro and in vivo applications. *Cosmetics* 2017;4(4):44.
- [57] van der Helm MW, Henry OYF, Bein A, Hamkins-Indik T, Crounce MJ, Leineweber WD, et al. Non-invasive sensing of transepithelial barrier function and tissue differentiation in organs-on-chips using impedance spectroscopy. *Lab Chip* 2019;19(3):452–63.
- [58] Cai EZ, Ang CH, Raju A, Tan KB, Hing EC, Loo Y, et al. Creation of consistent burn wounds: a rat model. *Arch Plast Surg* 2014;41(4):317–24.
- [59] Liang CC, Park AY, Guan JL. In vitro scratch assay: a convenient and inexpensive method for analysis of cell migration in vitro. *Nat Protoc* 2007;2(2):329–33.
- [60] Huang C, Ogawa R. Fibroproliferative disorders and their mechanobiology. *Connect Tissue Res* 2012;53(3):187–96.
- [61] Pacini S, Morucci G, Ruggiero M, Gulisano M, Punzi T. Tensegrity and plasma for skin regeneration. *Skin Res Technol* 2012;18(3):356–63.
- [62] Leask A. Ccn2: a mechanosignaling sensor modulating integrin-dependent connective tissue remodeling in fibroblasts? *J Cell Commun Signal* 2013;7(3):203–5.
- [63] Ma J, Zhao N, Zhu D. Bioabsorbable zinc ion induced biphasic cellular responses in vascular smooth muscle cells. *Sci Rep* 2016;6:26661.
- [64] Ma J, Zhao N, Zhu D. Biphasic responses of human vascular smooth muscle cells to magnesium ion. *J Biomed Mater Res A* 2016;104(2):347–56.
- [65] Day RM. Bioactive glass stimulates the secretion of angiogenic growth factors and angiogenesis in vitro. *Tissue Eng* 2005;11(5–6):768–77.
- [66] Sasaki Y, Sathi GA, Yamamoto O. Wound healing effect of bioactive ion released from Mg-smectite. *Mater Sci Eng C Mater Biol Appl* 2017;77:52–7.
- [67] Lamalice L, Le Boeuf F, Huot J. Endothelial cell migration during angiogenesis. *Circ Res* 2007;100(6):782–94.

- [68] Benam KH, Dauth S, Hassell B, Herland A, Jain A, Jang KJ, et al. Engineered in vitro disease models. *Annu Rev Pathol* 2015;10:195–262.
- [69] Lewis EEL, Barrett MRT, Freeman-Parry L, Bojar RA, Clench MR. Examination of the skin barrier repair/wound healing process using a living skin equivalent model and matrix-assisted laser desorption-ionization-mass spectrometry imaging. *Int J Cosmet Sci* 2018;40(2):148–56.
- [70] Miller LS. Toll-like receptors in skin. *Adv Dermatol* 2008;24:71–87.
- [71] Holland DB, Bojar RA, Farrar MD, Holland KT. Differential innate immune responses of a living skin equivalent model colonized by *Staphylococcus epidermidis* or *Staphylococcus aureus*. *FEMS Microbiol Lett* 2009;290(2):149–55.
- [72] Rademacher F, Simanski M, Harder J. RNase 7 in cutaneous defense. *Int J Mol Sci* 2016;17(4):560.
- [73] Singh D, Qi R, Jordan JL, San Mateo L, Kao CC. The human antimicrobial peptide LL-37, but not the mouse ortholog, mCRAMP, can stimulate signaling by poly(I:C) through a FPRL1-dependent pathway. *J Biol Chem* 2013;288(12):8258–68.
- [74] Yao C, Oh JH, Lee DH, Bae JS, Jin CL, Park CH, et al. Toll-like receptor family members in skin fibroblasts are functional and have a higher expression compared to skin keratinocytes. *Int J Mol Med* 2015;35(5):1443–50.
- [75] Chindera K, Mahato M, Sharma AK, Horsley H, Kloc-Muniak K, Kamaruzzaman NF, et al. The antimicrobial polymer PHMB enters cells and selectively condenses bacterial chromosomes. *Sci Rep* 2016;6:23121.
- [76] Xie Y, Yang L. Calcium and magnesium ions are membrane-active against stationary-phase *Staphylococcus aureus* with high specificity. *Sci Rep* 2016;6:20628.
- [77] Shalom A, Kramer E, Westreich M. Protective effect of human recombinant copper-zinc superoxide dismutase (hr-cuznsod) on intermediate burn survival in rats. *Ann Burns Fire Disasters* 2008;21(1):16–9.
- [78] Shalom A, Kramer E, Westreich M. Protective effect of human recombinant copper-zinc superoxide dismutase on zone of stasis survival in burns in rats. *Ann Plast Surg* 2011;66(6):607–9.
- [79] Lee Y, Kim MT, Rhodes G, Sack K, Son SJ, Rich CB, et al. Sustained Ca²⁺ mobilizations: a quantitative approach to predict their importance in cell-cell communication and wound healing. *PLoS One* 2019;14(4):e0213422.
- [80] Cogger V, Million N, Rehbock C, Sures B, Nachev M, Barcikowski S, et al. Tissue concentrations of zinc, iron, copper, and magnesium during the phases of full thickness wound healing in a rodent model. *Biol Trace Elem Res* 2019;191(1):167–76.
- [81] Palmieri B, Vadalà M, Laurino C. Nutrition in wound healing: investigation of the molecular mechanisms, a narrative review. *J Wound Care* 2019;28(10):683–93.
- [82] Shendi D, Marzi J, Linthicum W, Rickards AJ, Dolivo DM, Keller S, et al. Hyaluronic acid as a macromolecular crowding agent for production of cell-derived matrices. *Acta Biomater* 2019;100:292–305.
- [83] Chow O, Barbul A. Immunonutrition: role in wound healing and tissue regeneration. *Adv Wound Care (New Rochelle)* 2014;3(1):46–53.
- [84] Lange TS, Kirchberg J, Bielinsky AK, Leuker A, Bank I, Ruzicka T, et al. Divalent cations (Mg²⁺, Ca²⁺) differentially influence the beta 1 integrin-mediated migration of human fibroblasts and keratinocytes to different extracellular matrix proteins. *Exp Dermatol* 1995;4(3):130–7.
- [85] Broertjes J, Klarenbeek J, Habani Y, Langeslag M, Jalink K. TRPM7 residue S1269 mediates cAMP dependence of Ca²⁺ influx. *PLoS One* 2019;14(1):e0209563.
- [86] Evans KN, Potter BK, Brown TS, Davis TA, Elster EA, Forsberg JA. Osteogenic gene expression correlates with development of heterotopic ossification in war wounds. *Clin Orthop Relat Res* 2014;472(2):396–404.
- [87] Forsberg JA. Editor's spotlight/take 5: osteogenic gene expression correlates with development of heterotopic ossification in war wounds. *Clin Orthop Relat Res* 2014;472(2):393–5.
- [88] Wang G, Li Y, Li J, Zhang D, Luo C, Zhang B, et al. microRNA-199a-5p suppresses glioma progression by inhibiting MAGT1. *J Cell Biochem* 2019;120(9):15248–54.